AAPS PharmSciTech (2021) 22: 216
DOI: 10.1208/s12249-021-02099-3

Research Article

Eudragit S-100 Surface Engineered Nanostructured Lipid Carriers for Colon Targeting of 5-Fluorouracil: Optimization and *In Vitro* and *In Vivo* Characterization

Kruti Borderwala,[1] Sachin Rathod,[1] Sarita Yadav,[2] Bhavin Vyas,[1] and Pranav Shah[1,3]

Received 26 April 2021; accepted 19 July 2021; published online 12 August 2021

Abstract. 5-Fluorouracil (5-FU) is the most preferred chemotherapeutic agent in the management of colon cancer but is associated with poor therapeutic efficacy and lack of site specificity. Hence, it was aimed to employ Eudragit S100 surface engineered 5-FU nanostructured lipid carriers for the spatial and temporal release of the drug for the treatment of colon cancer. Hot high-pressure homogenization (HPH) technique was employed in the preparation of 5-FU-NLCs. The optimization of 5-FU-NLCs was performed using a Quality by Design (QbD) approach. A 3^2 factorial design was employed wherein the relationship between independent variables [amount of oleic acid (X_1) and concentration of Tween®80 (X_2)] and dependent variables [particle size (Y_1) and % entrapment efficiency (Y_2)] was studied. Optimized 5-FU-NLCs were surface treated to obtain Eudragit S100-coated 5-FU-NLCs (EU-5-FU-NLCs). The evaluation parameters for 5-FU-NLCs and EU-5-FU-NLCs included surface morphology, particle size, PDI, and zeta potential. *In vitro* release from EU-5-FU-NLCs revealed a selective and controlled 5-FU release in the colonic region for 24 h. *In vitro* cytotoxicity (MTT assay) was performed against Caco-2 cancer cells, wherein EU-5-FU-NLCs exhibited a 2-fold greater cytotoxic potential in comparison to a 5-FU solution (5-FU-DS). Oral administration of EU-5-FU-NLCs in Albino Wistar rats depicted a higher C_{max} (2.54 folds) and AUC (11 folds) as well as prolonged T_{max} (16 folds) and MRT (4.32 folds) compared to 5-FU-DS confirming higher bioavailability along with the spatial and temporal release in the colonic region. Thus, a multifaceted strategy involving abridgement of nanotechnology along with surface engineering is introduced for effective chemotherapy of colon cancer via oral administration of 5-FU with uncompromised safety and higher efficacy.

KEY WORD: S: 5-fluorouracil; nanostructured lipid carriers; Eudragit S100; colon targeting; colon cancer; bioavailability.

INTRODUCTION

Colon cancer is the second most common cancer diagnosed both in men and women with about 6–7 million deaths occurring globally every year (1,2). Among the available therapies for colon cancer, chemotherapy is preferred over surgery and radiation therapy (3). 5-FU is designated as the first-line therapy for early and advanced colon cancer (4). The currently available standard treatment of colon cancer includes intravenous injection of 5-FU either alone or in combination with other anti-cancer drugs (5). Upon IV administration, 5-FU exhibits (a) rapid achievement of plasma concentrations at a level much higher than the maximum safe level, resulting in serious side effects, and (b) quick drops in plasma concentration below the minimum effective concentration level, resulting in no therapeutic efficiency (6–8). 5-FU possesses a short life span (10–20 min) requiring frequent administration of the formulation to maintain the drug concentration above the minimum effective level as well as to provide desired therapeutic effect (9,10). This frequent administration by the invasive route results in poor patient compliance, development of resistance, systemic side effects, and drug distribution in higher amounts in normal tissues and organs (11). Peroral administration of 5-FU is convenient and patient compliant. Until date 5-FU oral tablets are not available, but recently Capecitabine (prodrug of 5-FU) tablets for oral administration has been approved by the USFDA. However, the oral formulations lack effectiveness

[1] Maliba Pharmacy College, Uka Tarsadia University, Bardoli, Gujarat 394350, India.
[2] Department of Pharmacy, Moti Lal Nehru Medical College, Prayagraj, Uttar Pradesh 211002, India.
[3] To whom correspondence should be addressed. (e–mail: pranav.shah@utu.ac.in)

due to the inability of the drug to reach the target site in effective concentrations due to first-pass hepatic and intestinal metabolisms. Additionally, oral administration is associated with great variability in pharmacokinetics resulting in unpredictable toxicity and efficacy (12,13). Therefore, the formulation scientists need to develop a delivery system for 5-FU that can be administered orally and can specifically target it to the colon and selectively release it at the tumor sites. Thus, a controlled drug delivery system along with the site specificity to the colon would provide reduced plasma drug fluctuations and systemic toxicity along with the efficacy and safety of the drug. Eudragit S100, a pH-sensitive polymer, has been found to provide release in the colonic region at around pH 6.5-7.5 (14). Nanoparticles are known to provide avoidance of first-pass metabolism and sustain the release (15,16). Hence, a combination of nanotechnology along with surface modification by Eudragit S100 would serve the desired purpose.

Subudhi et al. (15) developed 5-FU-loaded citrus pectin nanoparticles and coated them with Eudragit S100 (E-CPNs) with the aim of colon targeting. The targeting ability of E-CPNs to cancer cells could be inferred based on the *in vitro* and *in vivo* studies. Tummala et al. (2015) prepared 5-FU-loaded chitosan polymeric nanoparticles by solvent-evaporation emulsification technique (17). The *in vitro* studies exhibited major release in a sustained fashion at the colonic pH of 7.0. Tummala et al. (17) developed 5-fluorouracil enteric-coated nanoparticles and evaluated their apoptotic activity *in vitro* on HCT 116 colorectal cancer cell lines and *in vivo* on xenograft models in nude mice (4). Sutar et al. (18) developed Eudragit S100-coated PLGA nanoparticles containing 5-FU for colorectal cancer therapy. The authors studied the *in vitro* release and *in vitro* cytotoxicity (HT-29 cell lines) of the developed formulation. 5-FU NLCs have been employed for hepatocellular carcinoma (19), gastric cancer (20), skin cancer (21), etc. However, there are no reports in the literature regarding the employment of NLCs or Eudragit S100-coated NLCs for 5-FU delivery for colon cancer. NLCs are an advanced version (second generation) of solid lipid nanoparticles. NLCs comprise liquid lipids in addition to solid lipids and thus provide a highly disordered structure that increases its capacity for drug loading. The other merits associated with NLCs include higher stability, modulation of release, low cost, and ease for scaling up (22,23). Hence, the study aimed at developing Eudragit S100-coated NLCs for delivery of 5-FU to the colon. 5-FU-NLCs were synthesized using HPH technique and optimized using 3^2 full factorial design. Critical material attributes such as the amount of oleic acid (liquid lipid) and concentration of Tween®80 (surfactant) were included as independent variables to study influences on dependent variables such as particle size and encapsulation efficiency. The optimized 5-FU-NLCs were further surface coated with pH-dependent polymer-Eudragit S100 to get EU-5-FU-NLCs. The developed formulation was characterized in terms of *in vitro* and *ex vivo* drug release, stability, surface morphology, *in vitro* cytotoxicity on Caco-2 cell lines, and *in vivo* pharmacokinetic studies.

MATERIALS AND METHODS

5-FU was a generous gift sample from Celon Lab Pvt. Ltd. (Hyderabad, India). Precirol®ATO5 (glyceryl palmitostearate), Compritol®ATO 888 (glyceryl dibehenate), Labrafac™ PG (propylene glycol dicaprylocaprate), and Labrafil™ M1944CS (oleoyl polyoxyl-6 glycerides) were kindly provided by Gattefossé India (Mumbai, India). Glyceryl monostearate (GMS), oleic acid, stearic acid, isopropyl myristate (IPM), Tween®20 (polyoxyethylene sorbitan monolaurate), Tween®80 (polyoxyethylene sorbitan monooleate), and n-butanol were purchased from Loba Chemie (Mumbai, India). Eudragit S100 was procured as a gratis sample from Evonik Degussa India Pvt. Ltd. (Mumbai, India). All other chemicals used were of analytical grade. Milli-Q water (Merck Life Sciences, USA) was used throughout the study wherever needed. *Screening of Solid Lipid.* Solubility of 5-FU in solid lipid is a crucial factor that determines the encapsulation efficiency of the active. Since equilibrium solubility studies could not be carried out in this case, a modified method was employed (22). Stearic acid, Precirol®ATO 5, Compritol®ATO 888, and GMS were screened for their potential to solubilize 5-FU. Ten milligrams of 5-FU were placed in a screw-capped glass vial. Each lipid was separately heated at 10°C above its melting point, on a temperature-regulated water bath (Macro Scientific Work Pvt. Ltd., Delhi, India). The gradual addition of the molten lipid was done to the 5-FU vial with continuous stirring until the formation of a clear solution. The quantity of lipid required to solubilize 5-FU was recorded. Among the various lipids, the one that could solubilize the fixed amount of 5-FU with the lowest amount was selected. The experiment was performed in triplicate.

Screening of Liquid Lipid. Liquid lipid also plays a crucial role in the entrapment of the active. Labrafac™ PG, Labrafil™ M1944CS, oleic acid, and IPM were screened to determine the maximum solubility of 5-FU. Briefly, an excess amount of 5-FU was added to screw-capped glass vials containing 10 mL of liquid lipid followed by mixing on a vortex mixer for 10 min. Further, the vials were placed in an isothermal orbital shaker maintained at 25 ± 2°C for 24 h. Centrifugation was carried out at 4°C at 20000 rpm for 30 min. The supernatant (3 mL) was separated, filtered, and analyzed spectrophotometrically at 266 nm (24).

Screening of Surfactants. Surfactants were screened based on maximum solubility of 5-FU in Tween®20, Tween®80, and n-butanol. An excess amount of 5-FU was taken in screw-capped glass vials containing 10 mL of surfactant. Mixing was carried out on a vortex mixer for 10 min followed by shaking in an isothermal orbital shaker at 25 ± 2°C for 24 h. The vials were centrifuged at 4°C at 20000 rpm for 30 min, and the supernatant (3 mL) was analyzed spectrophotometrically at 266 nm (24).

Selection of Excipients for 5-FU-NLCs. Based on the screening studies, Compritol®ATO 888, oleic acid, and Tween®80 were selected as solid lipid, liquid lipid, and surfactant, respectively, for further batches. This composition makes the formulation quite novel and unique. Both oleic

acid and Tween®80 are classified as food additives, whereas Compritol®ATO 888 is a generally recognized as safe (GRAS) excipient. These materials are low cost, non-toxic, safe for enteral human use, and have been used in pharmaceutical, food, and cosmetic industries with no signs of toxicity.

Design of Experiments. 3^2 factorial design was employed to study the relationship between independent variables (amount of oleic acid and concentration of Tween®80) and responses (mean particle size and % entrapment efficiency) of the prepared formulations. Each independent variable was employed at three levels [−1 (low), 0 (medium), and +1 (high)]. Independent variables and levels used for the optimization of 5-FU-NLCs are depicted in Table I. Interactive multiple regression analysis and F statistics were employed to evaluate the responses. The regression equation for the response is given below:

$$Y = b_0 + b_1X_1 + b_2X_2 + b_{12}X_1X_2 + b_{11}X_1^2 + b_{22}X_2^2 \quad (1)$$

where Y is the measured response, b_0 is the intercept, and b_1 and b_2 represent the regression coefficients for the polynomial equations. X_1 and X_2 are the independent variables. ${X_1}^2$ or ${X_2}^2$ indicates the quadratic effects of the variables. X_1X_2 represents the interactions between two factors. Multiple regressions were applied using Design Expert Software (Version 11.0.7.1, Stat-Ease, Inc., Minneapolis, MN, USA) to deduce the variables having a significant effect on the responses. The variables having a P-value < 0.05 in the model were considered to contribute significantly to the recorded response (25).

Method of Preparation of 5-FU NLCs. HPH technique was employed in the preparation of 5-FU-NLCs (26). The preparation of the lipidic phase involved melting of Compritol®ATO 888 (250 mg) and mixing different amounts of oleic acid at 80°C followed by adding 5-FU (50 mg) to it. The aqueous phase (10 mL) was prepared by different concentrations of Tween®80 maintained at identical temperatures. In the next step, the lipidic phase was dispersed into the aqueous phase at 10000 rpm for 2 min. The coarse emulsion was homogenized [AH-100D high-pressure homogenizer (ATS Engineering Limited, China)] applying three cycles at a pressure of 600 bars. Upon cooling the resultant o/w nanoemulsion at an ambient temperature, lipid phase recrystallization occurred leading to the formation of 5-FU-NLCs.

Characterization of 5-FU-NLCs

Mean Particle Size, Pdi, and Zeta Potential. The mean particle size, PDI, and zeta potential (ZP) were determined at 25°C by a Zeta-Sizer (Nano ZS 90, Malvern Ltd., UK) after being diluted 10 times with Milli-Q water. Each sample was measured in triplicate, and the values are expressed as the mean diameter ± standard deviation (17,27).

Entrapment Efficiency. The entrapment efficiency (% EE) is defined as the percentage of the active encapsulated in respect to the total amount of the active used to prepare the nanoformulation. The amount of 5-FU entrapped within the 5-FU-NLCs was determined by measuring the amount of non-entrapped 5-FU (28). Briefly, 5 mL of the nanodispersion was centrifuged (REMI C24 Plus, Remi Instruments, Vasai, India) at 25,000 rpm for 30 min at 4°C. The collected supernatant (2 mL) was collected and was analyzed using UV-1800 Shimadzu spectrophotometer (Shimadzu Corporation, Kyoto, Japan), at a λ_{max} of 266 nm.

$$\%EE = \frac{Added\ drug - free\ drug}{Added\ drug} \times 100 \quad (2)$$

In Vitro Drug Release Study. In vitro release profiles of 5-FU from the 5-FU-DS and 5-FU-NLCs were obtained by a dialysis bag technique (29). The release media employed were as follows: pH 1.2 (indicative of gastric fluid) for the first 2 h, pH 4.5 (indicative of intestinal fluid) for the next 4 h, and pH 7.4 (indicative of colonic fluid) for the remaining 18 h. The pH variation was carried out to mimic mouth-to-colon transit as well as to determine the effect of different pH on drug release and localization. Five milliliters of 5-FU DS or 5-FU-NLCs (equivalent to 50 mg of 5-FU) were introduced into dialysis bags prepared from preactivated dialysis membrane (Himedia-Dialysis membrane 135, Mol. cut off 3.5 KDa, Mumbai, India). The bag was immersed into a beaker comprising of 50 mL of release media, which was stirred at 50 rpm using a magnetic stirrer. The temperature of the receptor compartment was maintained at 37 ± 1°C. Aliquots of release medium (3 mL) were withdrawn at a predefined time intervals and replaced with fresh release medium to maintain sink conditions. The collected samples (3 mL) were analyzed spectrophotometrically at 266 nm. Blank formulations were employed for base correction to nullify the effect of excipients used in the formulation. All release experiments were performed in triplicate.

Generation of Polynomial Equations and Response Surface Plots. Various response surface methodology (RSM) computations for the current optimization study were performed employing Design-Expert software. Polynomial models including quadratic terms were generated for all the response variables. In addition, 3D graphs were constructed using the output files generated by the Design-Expert software. The significance of these parameters on the variables was assessed by analysis of variance (ANOVA) (25).

Constrained and Graphical Optimization of 5-FU-NLCs. To find the best formulation, a numerical optimization technique based on desirability function was employed (25). The constraints on the responses of 5-FU-NLCs included (i) particle size (Y_1) below 200 nm and (ii) entrapment efficiency greater than 80% (Y_2). The solutions generated by the Design-Expert software were sorted in the descending order of the desirability, and the formulation with the highest desirability factor (values close to 1) was considered for

Table I. Effects of Independent Variables (Coded and Decoded) on Dependent Variables in 3^2 Full Factorial Design for 5-FU-NLCs

Formulation code	Amount of oleic acid (mg) [X_1]		Conc. of Tween 80 (%w/v) [X_2]		Particle size (nm) [Y_1]	% EE [Y_2]
	Coded	Decoded	Coded	Decoded		
NLC-1	−1	25	−1	0.5	333.4 ± 10.73	60.84 ± 1.5
NLC-2	0	50	−1	0.5	317.3 ± 10.29	78.30 ± 1.9
NLC-3	+1	75	−1	0.5	285.8 ± 8.64	92.12 ± 2.2
NLC-4	−1	25	0	1.0	224.9 ± 6.55	55.43 ± 2.0
NLC-5	0	50	0	1.0	189.3 ± 7.10	73.56 ± 2.7
NLC-6	+1	75	0	1.0	160.1 ± 7.92	88.71 ± 2.1
NLC-7	−1	25	+1	1.5	192.4 ± 10.63	51.68 ± 1.9
NLC-8	0	50	+1	1.5	141.3 ± 10.29	70.09 ± 2.5
NLC-9	+1	75	+1	1.5	98.6 ± 7.71	85.27 ± 2.8

 # Particle size: NMT 200 nm
% EE: NLT 80%

further formulation. Graphical optimization was performed by applying constraints to generate design space.

Validation of Experimental Design. 3^2 factorial design employed for the fabrication of 5-FU-NLCs was further validated by checkpoint analysis. An optimized batch of 5-FU-NLCs was formulated based on the values of independent variables obtained from the desirability function and overlay plot. Experimental and predicted values of the responses were compared to confirm the validity of the design (25).

Surface Modification of 5-FU-NLCs. Optimized batch of 5-FU-NLCs was subjected to enteric coating with Eudragit S100 solution to protect the active from getting released in the stomach or upper part of the GIT and thereby allowing the major amount of 5-FU to get released in the colon. Briefly, Eudragit S100 (100 mg) was dissolved in a mixture (10 mL) of methanol/water (2:1). The obtained 5-FU-NLCs dispersion (2 mL) was further added drop wise to above prepared polymeric solution (10 mL), with constant stirring at 900 rpm for 12 h at room temperature (15).

5-FU-NLCs/EU-5-FU-NLCs were lyophilized using a programmable freeze-dryer (FreeZone 2.5-L Benchtop Freeze Dryer, Labconco, Mumbai, India). For lyophilization, 2 mL 5-FU-NLCs/EU-5-FU-NLCs dispersion and 2 mL 3% w/v mannitol were introduced into vials. The freezing was carried out at −50°C for 48 h followed by primary drying at −30°C and 150 mTorr for 24h. The last step consisted of secondary drying at 22°C and 50 mTorr for 6 h (30). The lyophilized EU-5-FU-NLCs contained 50 mg of 5-FU per gram of EU-NLCs.

Evaluation of Optimized 5-FU-NLCs and EU-5-FU-NLCs

Attenuated Total Reflectance Fourier Transform Infrared Spectroscopy (ATR-FTIR). The samples of 5-FU, Compritol®ATO 888, oleic acid, Tween®80, Eudragit S 100, physical mixture, 5-FU-NLCs, and EU-5-FU-NLCs were placed on the glass window of FTIR (Bruker Optics Alpha, Mumbai, India). The intensity peaks vs. wavenumbers ranging from 4000 to 500 cm^{-1} were recorded, identified, and interpreted (31).

Differential Scanning Calorimetry. A differential scanning calorimeter (STA PT-1600, Linesis Inc., NJ, USA) was employed to observe the melting and the phase transition behavior of 5-FU (pure drug) and EU-5-FU-NLCs. Five milligrams of the individual samples were accurately weighed using a microbalance (MC5, Sartorius, Germany), sealed in the aluminum DSC pans and placed over the sample platform. The pans were heated from 25 to 300°C at the rate of 10°C/min under nitrogen purging (20 mL/min) (32).

Particle Morphology. The morphology of 5-FU-NLCs and EU-5-FU-NLCs was studied by SEM (JEM 100-CX; JEOL, Tokyo, Japan). For analysis, a double-adhesive tape was applied to an aluminum stub. Then, 1–2 drops of NLCs dispersions were dropped on the stub and left to dry overnight at room temperature in a desiccator. The stubs were gold coated to a thickness of ~250 Å under an inert argon atmosphere using a gold sputter coater in a high-vacuum evaporator. The coater was operated at 0.1 torrs (argon) for 90 s at an accelerating voltage of 15 kV. The coated samples were then scanned, and photomicrographs were taken at suitable magnification. The analysis was performed at 25 ± 2°C (33).

X-ray Diffraction Analysis. Diffractograms of 5-FU and EU-5-FU-NLCs were recorded by X-ray diffractometer (DX178 2700, China) in symmetrical reflection mode using Cu Kα radiation generated at 30mA and 40 kV. The scanning speed was 10°C/min from 0° to 55°of 2θ (34).

% EE: % EE of 5-FU-NLCs and EU-5-FU-NLCs were performed as described in the previous section.

Mean Particle Size, PDI, and Zeta potential. Particle size, PDI, and zeta potential of 5-FU-NLCs and EU-5-FU-NLCs were performed as described in the previous section.

In Vitro Release Study. In vitro release of 5-FU-NLCs and EU-5-FU-NLCs were performed as described in the previous section.

Ex Vivo Release Study. The *ex vivo* study was approved by the Institutional Animal Ethics Committee, Maliba Pharmacy College, India (MPC/IAEC/17/2018). The non-everted gut sac method was used to conduct *ex vivo* release of 5-FU-DS and EU-5-FU-NLCs (35). Male Albino Wistar rats weighing 200 ± 20 g were utilized in the investigation and sacrificed using a higher dose of anesthesia. The colon was excised and placed immediately in oxygenated Krebs Ringer phosphate buffer saline (pH 7.4). The circular and longitudinal muscle layers were stripped manually. Using a syringe with a blunt end, the colon was gently rinsed out with cold normal oxygenated saline solution (0.9% w/v, NaCl). The sac was loaded with 2 mL of EU-5-FU-NLCs (equal to 50 mg of 5-FU) using a blunt needle after one end was tied, keeping the effective sac length at 6 cm for release study. In a glass conical flask containing 50 mL of Krebs Ringer phosphate buffer saline (pH 7.4), each sac was inserted. In a water shaker bath rotating at 50 rpm, the entire system was kept at 37 ± 1.0°C and gassed with oxygen (10–15 bubbles per minute) using a laboratory aerator. Two-milliliter samples were taken from outside the sacs and replaced with 2 mL of fresh release media at predetermined time intervals. A UV-visible spectrophotometer was used to analyze the samples at 266 nm. Similarly, a release study was performed using blank EU-NLCs (without drug), and the absorbance values were subtracted from the test to account for the effect of excipients.

The obtained results were fitted into various mathematical models such as zero order, first order, Higuchi, Hixon-Crowell, and Korsmeyer-Peppas models for evaluation of kinetics and mechanism of drug release (36).

In Vitro Cytotoxicity Assay. In vitro cytotoxicities of Eudragit S100-coated blank NLCs, 5-FU-DS, 5-FU-NLCs, and EU-5-FU-NLCs were performed by MTT assay. Caco-2 cells were seeded onto 96 well plates at a seeding density of 5×10^3 cells/well and maintained at 37°C in 95% humidity and 5% CO_2 environment. The cells were incubated for 21 days to allow cell attachment during which media change was done on alternate days. The media was removed and samples of 5-FU-DS, 5-FU-NLCs, and EU-5-FU-NLCs at different concentrations (1, 10, and 100 μM) were added to the cells and incubated for 72 h. Blank EU-NLCs were considered as control. Post-treatment, the cells were washed two times with phosphate buffer solution. This was followed by the addition of 20 μL of the MTT solution (5 mg/mL in phosphate buffer solution) to each well followed by incubation at 37°C in a 5% CO_2 environment. After 4 h, 100 μL of dimethyl sulfoxide was added to each well to dissolve the formazan crystals followed by measurement of absorbance at λ_{max} of 550nm using a microplate reader (Thermo Scientific, Pittsburgh, USA). The experiment was carried out in triplicate in parallel (4).

Bioanalytical Method Development for the Estimation of 5-FU in Plasma. 5-FU concentration in plasma was determined using HPLC system (Shimadzu LC-2010-CHT, Japan) consisting of a binary pump (LC20AT) and injection (Rheodyne, 20-μL loop) with UV detector connected to a computer having LC solution software Version. 1.25. The chromatographic separation was carried out using a C-18 reverse phase GraceSmart column (250 mm × 4.6 mm; 5 μm). Mobile phase comprising of 50 mM KH_2PO_4 (pH 5 ± 0.1) was isocratically pumped at 1 ml/min. The injection volume was 20 μL, and the detection wavelength was 254 nm. The mobile phase was sonicated for 15 min and filtered through a 0.45-μm membrane filter before use. 0.2 mL of the plasma samples containing 5-FU were extracted with 2 mL of isopropyl alcohol. The precipitated protein was removed by centrifugation at 20000 rpm for 10 min at 4°C. The supernatant was separated and evaporated to dryness by purging N_2 gas at room temperature. The dried sample was reconstituted with a 0.3-mL mobile phase and evaluated by HPLC for determining the amount of 5-FU (37).

In Vivo Study. Eighteen male Albino rats of Wistar strain (200 ± 20 g) were randomly divided into three groups (six animals each). The study was approved by the Institutional Animal Ethics Committee, Maliba Pharmacy College, India (MPC/IAEC/17/2018). They were acclimatized in well-spaced ventilated cages at a 22 ± 2°C/65 ± 5% RH under natural light/dark conditions for 7 days and free access to standard diet and water. The animals were fasted overnight before experiments with water *ad libitum*. 5-FU-DS, 5-FU-NLCs, and EU-5-FU-NLCs were administered orally to the rats in a single administration by using an oral cannula at a 5-FU dose of 10 mg/kg. Group 1 received 5-FU-DS, group 2 received 5-FU-NLCs, whereas group 3 received EU-5-FU-NLCs. 0.1 mL of blood samples were withdrawn from the retroorbital plexus of the rats using uniformly tapered capillary at the predetermined time points (0.25, 0.5, 1, 2, 3, 4, 6. 8, 12, 24 h). Samples were collected in microcentrifuge tubes containing EDTA (1.8 mg per mL of blood) and were separated by centrifugation at 20000 rpm for 10 min at 4°C and stored at –20°C until analysis. The extraction of 5-FU from plasma samples was carried out by extraction technique as described earlier followed by its estimation using the HPLC method.

The pharmacokinetic parameters, namely T_{max}, mean residence time (MRT), maximum plasma concentration (C_{max}), and area under the plasma concentration-time curve [(AUC_{0-t}) and ($AUC_{0-\infty}$)], were calculated using PKSolver software (Microsoft Excel, USA) (15).

Stability Study. EU-5-FU-NLCs were evaluated for their storage stability at different temperature conditions. EU-5-FU-NLCs were sealed and stored in airtight glass vials at 4 ± 2°C in refrigerator and 25 ± 2°C/60 ± 5% RH, for 1 month. Particle size and entrapment efficiency were determined at predetermined intervals (0, 10, 20, and 30 days).

Statistical Analysis. All results were expressed as mean ± standard deviation (SD). Statistical analysis was performed using Student's t-test, and statistical significance was designated as $P<0.05$.

RESULTS AND DISCUSSION

Preliminary Screening Studies. Preliminary screening studies were carried out to identify the material attributes

influencing the development of 5-FU-NLCs. Lipids are of prime importance in influencing drug entrapment efficiency, particle size, and drug release profile. Hence, choosing suitable lipids is crucial in the fabrication of 5-FU-NLCs (38). Different solid lipids, namely stearic acid, Compritol®ATO 888, Precirol® ATO5, and GMS, were evaluated for their solubilizing ability of 5-FU. Based on the solubility studies (Fig. 1a) and reported biocompatibility and safety, Compritol®ATO 888 was chosen for the fabrication of 5-FU-NLCs in the present study. Liquid lipids are also vital in deciding the entrapment of drugs in NLCs. From Fig. 1b, it is clear that 5-FU has maximum solubility in oleic acid (7.76 ± 0.45 mg/mL) as compared to isopropyl myristate (0.107 ± 0.01 mg/mL), Labrafil™ M1944 CS (3.42 ± 0.91 mg/mL), and Labrafac™ PG (0.319 ± 0.03 mg/mL). Therefore, oleic acid was selected as a liquid lipid to form a matrix with solid lipid-Compritol®ATO 888 for the development of 5-FU-NLCs. Various surfactants like Tween®20, Tween®80, and butanol were also screened based on the solubility of 5-FU. The solubilities of 5-FU in Tween®20, Tween®80, and butanol were 6.156 ± 1.75 mg/mL, 24.876 ±3.58 mg/mL, and 2.79 ± 0.72 mg/mL, respectively (Fig. 1c). Hence, Tween®80 was selected as a surfactant for further studies.

Based on the preformulation studies (data not shown), the amount of oleic acid and concentration of Tween®80 were identified as critical material attributes affecting the particle size and entrapment efficiency of 5-FU-NLCs. Hence, they were employed as independent variables in the 3^2 factorial design.

Factorial Design. A 3^2 full factorial design was employed to study the interplay between independent and dependent variables (39). Using the amount of oleic acid (X_1) and concentration of Tween®80 (X_2) as independent variables, 9 batches of 5-FU-NLCs were formulated by HPH method. The coded and decoded values of independent variables for different batches along with the values of responses—MPS (Y_1) and % EE (Y_2)—are shown in Table I. The responses of the formulated batches were recorded, and the data was subjected to multiple linear regressions for the generation of polynomial models [linear, two-factor interaction (2FI) and quadratic]. Based on the R^2 value (Table S1), the quadratic model was found to be the most suitable for Y_1 and Y_2. The p values for the quadratic models of Y_1 and Y_2 were found to be 0.0002 and < 0.0001, respectively, indicating the models to be significant and their ability to establish a correlation between independent variables and responses.

Effect of Independent Variables on Mean Particle Size. The mean particle size of the formulated 5-FU-NLCs was recorded in the range of 98.6 to 333.4 nm. Based on the R^2 value, the "quadratic" model was found to be significant for MPS, and the lack of fit was insignificant. The model F value obtained for MPS was 453.54 which implies that there is only a 0.02% chance that it may be due to noise. ANOVA was performed to identify the significance of each independent variable on the response. The variables possessing a P value < 0.05 are considered to be significant. The R^2, adjusted R^2, and predicted R^2 values were 0.9987, 0.9965, and 0.989. The recorded adequate precision value was 60.1703 which is

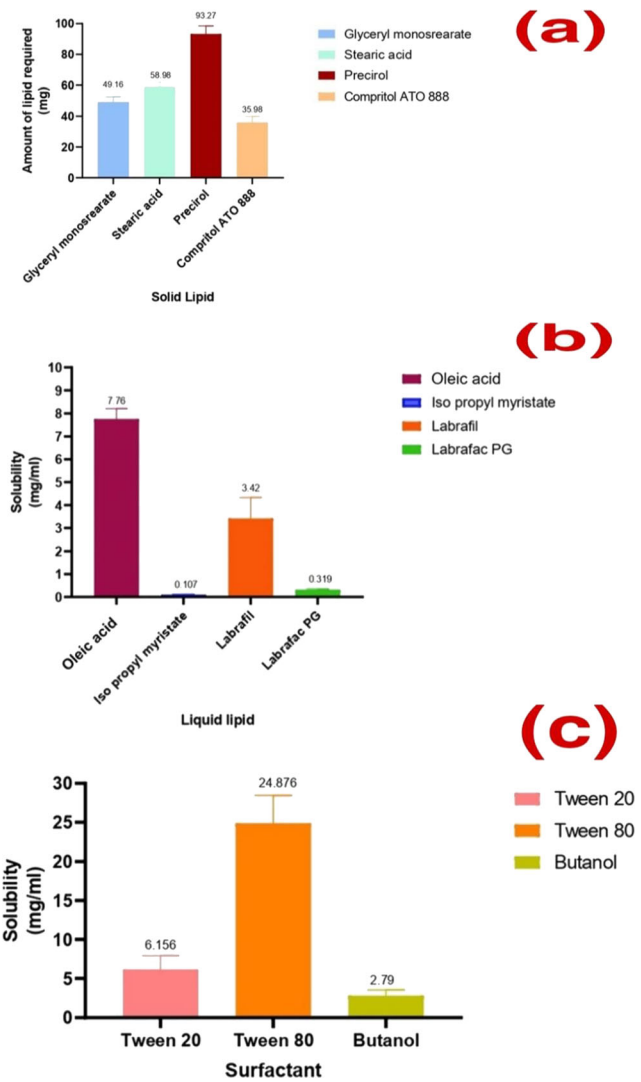

Figure 1. a Amount of solid lipid (mg) required to solubilize 5-FU. b Solubility of 5-FU in liquid lipids. c Solubility of 5-FU in surfactants

>4, indicating high signal-to-noise ratio and the capability of the model to explore the design space (25). The P values of the terms X_1, X_2, X_1X_2, and X_2^2 were < 0.05 indicating their significant role in influencing MPS (Table S2). Hence, these terms are considered significant, and the resultant reduced equation was

$$Y1\,(MPS) = 191.50 - 34.37X1 - 84.03X2 - 11.55X1X2 - 0.10X12 + 36.70X22 \quad (3)$$

The effect of each independent variable on the mean particle size is explained by Equation 3 and also explained graphically by 3D response surface plots (Fig. 2a). As seen in the equation, the negative sign associated with X_1 and X_2 indicates an antagonistic effect on Y_1, i.e., a decrement in particle size when the amount of oleic acid and concentration of Tween®80 is increased. The coefficients for X_1 and X_2 were found to be 34.37 and 84.03, respectively, indicating concentration of Tween®80 to be a major contributing factor affecting the particle size of 5-FU-NLCs in comparison to the

amount of oleic acid. The decrement in particle size may be attributed to the reduction in surface tension caused by Tween®80, leading to the formation of smaller nanoparticles. Additionally, it forms a dense network around the nanoparticles and provides steric hindrance to agglomeration (38). The particle size of 5-FU-NLCs was found to decrease when the amount of oleic acid increased from 25 to 75 mg. The decrease in particle size may be attributed to the exclusion of oleic acid during particle formation. As the system is cooled, Compritol®ATO 888 (solid lipid) re-crystallizes and rearranges itself to form the core of the NLCs. On the other hand, oleic acid may remain outside or might be randomly distributed due to its soft structure resulting in a liquid-lipid free core or a core with little lipid (40).

Effect of Independent Variables on % EE. % EE is a number that is a quantitative representation of the amount of the drug that is encapsulated into nanoparticles. The % EE of the prepared 5-FU-NLCs was in the range of 51.68 to 92.12%. The "quadratic" model suggested for % EE by the design software was found to be significant, and the lack of fit was found to be insignificant. The obtained *F* value for % EE was 3731.80 suggesting that there is only a 0.01% chance that it may be due to noise. ANOVA was performed to identify the significance of each independent variable on % EE. Independent variables with a *P* value < 0.05 are considered to be significant. The R^2, adjusted R^2, and predicted R^2 values were 0.9998, 0.9996, and 0.9981. The obtained adequate precision was 164.9978 which is > 4, indicating a high signal-to-noise ratio and the capability of the model in exploring the design space (25). The *P*-values of the terms X_1, X_2, X_1X_2, and X_1^2 were recorded< 0.05, indicating their significant role in influencing % EE (Table S3). Hence, these terms are considered significant, and the resultant reduced equation was

$$Y2\ (\%EE) = 73.66 + 16.36X1\text{–}4.04Y2 + 0.58X1X2\text{–}1.64X12 + 0.48X22 \quad (4)$$

Equation 4 and the 3D response surface plots (Fig. 2b) provide information pertaining to the influence of each variable on the % EE. As seen in Equation 4, the positive sign associated with X_1 indicates a synergistic effect, whereas the negative sign associated with X_2 indicates an antagonistic effect on Y_2, i.e., an increment in %EE when the amount of oleic acid is increased from 25 to 75 mg and decrement in % EE when the concentration of Tween®80 is increased from 0.5 to 1.5%. The coefficients for X_1 and X_2 were found to be 16.36 and 4.04, respectively, indicating the amount of Oleic acid to be a major contributing factor affecting the % EE of 5-FU-NLCs in comparison to the concentration of Tween®80. Since 5-FU has a greater solubility in oleic acid, an increment in its amount increases the solubilization of 5-FU leading to the incorporation of more amount of active. Additionally, the entropy of oleic acid, which is a less ordered lipid, provides more space for the entrapment of 5-FU molecules. The observation of an increase in %EE with an increase in the amount of liquid lipid was in accordance with previously reported work (40,41). Another factor influencing %EE was the concentration of Tween®80. As the concentration of Tween®80 is increased, it leads to the formation of mixed micelles, which show co-existence with NLCs, resulting in decreased entrapment of 5-FU within the lipidic nanoformulation. Here, mixed micelle consists of 5-FU and Tween®80; therefore, availability of the active for NLC decreases. Also, micellar solubilization of 5-FU and surface modifying property of Tween®80 influence porosity of the lipid matrix, facilitating the diffusion of 5-FU to the external phase and thus accounting for decreased 5-FU encapsulation. The observation of a decrease in %EE with an increase in surfactant was in accordance with previously reported work (38,42).

Optimization and Validation. The optimization process for 5-FU-NLCs was carried out by determining the optimal experimental values, which were obtained by solving the determined polynomial regression equations and grid searching in the overlay plot (Fig. 2c) applying the following criteria: particle size-NMT 200 nm (Y_1) and EE-NLT 80% (Y_2). The optimum levels of the independent variables (formulation factors) are presented in Table II. A formulation checkpoint batch was designed and formulated according to the regression equation and overlay plot to validate their liability and the precision of the factorial design, using these optimal experimental conditions. The checkpoint formulation was evaluated for MPS and % EE (Table II), and the recorded responses were compared with the predicted values.

The optimized batch of 5-FU-NLCs was coated with Eudragit S100 to obtain EU-5-FU-NLCs.

Mean Particle Size, PDI, and ZP of Optimized 5-FU-NLCs and EU-5-FU-NLCs. The MPS, PDI, and ZP of 5-FU-NLCs and EU-5-FU-NLCs were determined, and their values are represented in Table II. 5-FU-NLCs displayed MPS 101.7 ± 1.32 nm, whereas EU-5-FU-NLCs exhibited MPS of 154.0 ± 3.17 nm. The increase in the size of EU-5-FU-NLCs could be attributed to the surface covering of 5-FU-NLCs (uncoated) by Eudragit S100 (15). PDIs of 5-FU-NLCs and EU-5-FU-NLCs were found to be 0.27 ± 0.02 and 0.29 ± 0.07, respectively, indicating homogenous size distributions for the uncoated as well as coated nanoparticles.

ZP is an indicator of the stability of colloid dispersions, wherein a high ZP value leads to an electric repulsion among particles, thereby avoiding their aggregation (29). ZP of 5-FU-NLCs and EU-5-FU-NLCs were found to be (−8.19) ± 1.03 mV and (−21.7) ± 2.02 mV, respectively. The higher ZP of EU-5-FU-NLCs could be attributed to free acrylic acid groups present on the surface of the anionic polymer-Eudragit S100.

% EE of Optimized 5-FU-NLCs and EU-5-FU-NLCs. % EE of 5-FU-NLCs and EU-5-FU-NLCs were found to be 83.50 ± 2.4% and 89.81 ± 2.6%, respectively. The higher entrapment observed in EU-5-FU-NLCs could be due to an additional coating that minimizes the leakage of 5-FU from NLCs (43).

Morphology. SEM images of 5-FU-NLCs (Fig. 3a) and EU-5-FU-NLCs (Fig. 3b) indicate that the particles were of nanometric size range and spherical shape. The sizes of the

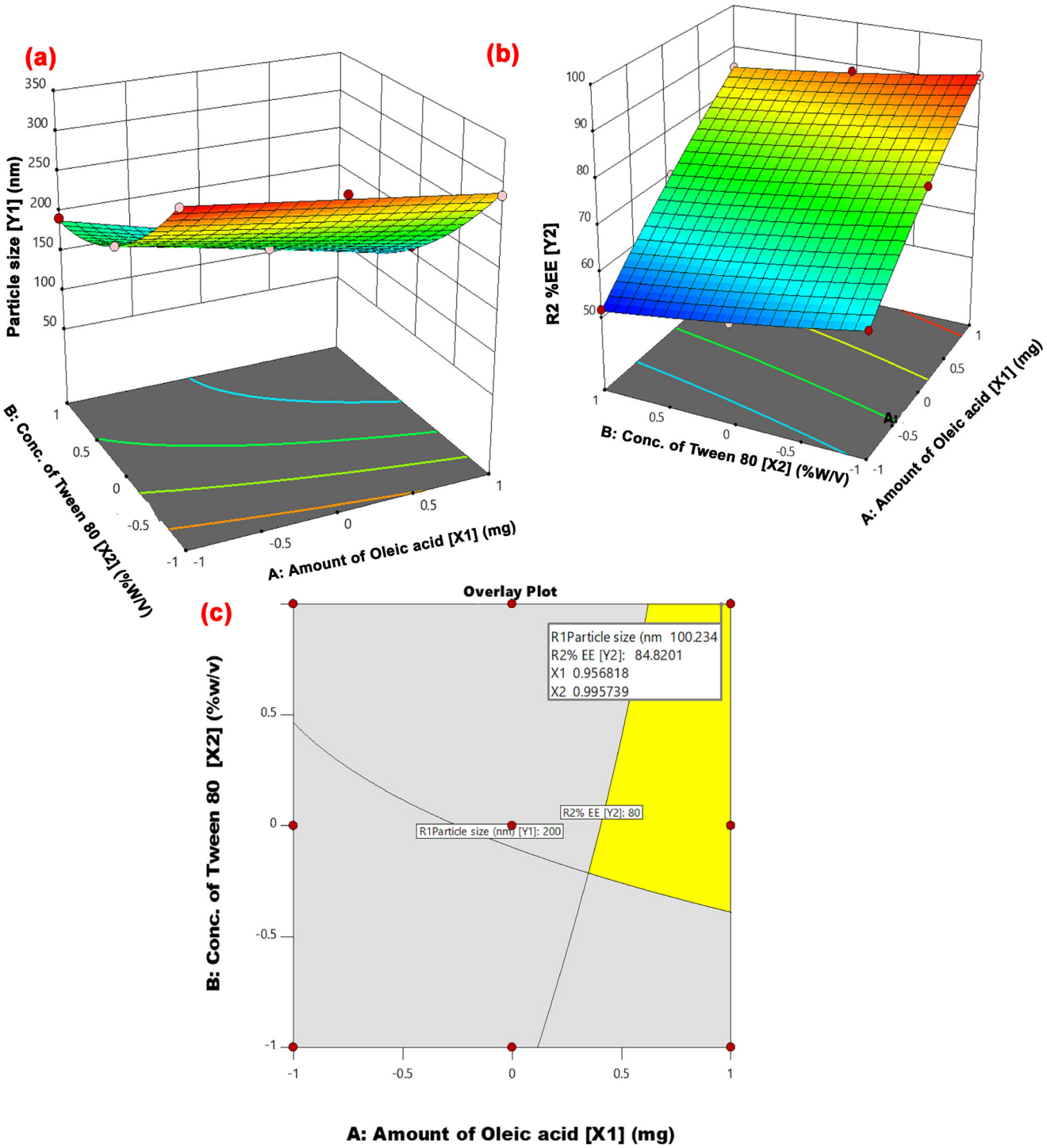

Figure 2. **a** 3D response surface plot showing the influence of amount of oleic acid (X_1) and concentration of Tween 80 on particle size. **b** 3D response surface plot showing the influence of amount of oleic acid (X_1) and concentration of Tween 80 (X_2) on %EE. **c** Overlay plot of 3^2 factorial design showing the desirable region for selection of optimized 5-FU-NLCs

particles observed in the SEM images are in good agreement with the data obtained from DLS (Table I).

Attenuated Total Reflectance Fourier Transform Infrared Spectroscopy. To evaluate the presence of any possible drug-excipient interactions, 5-FU, Compritol®ATO 888, oleic acid, Tween®80, Eudragit S100, physical mixture, 5-FU-NLCs, and EU-5-FU-NLCs were scanned in the range of 4000–400 cm^{-1} (Fig. 4). 5-FU exhibited characteristic peaks at 3065, 1640, and 1273 cm^{-1} (16). Compritol®ATO 888 showed peaks at 2922, 1707, and 1592 cm^{-1}, whereas oleic acid displayed characteristic peaks at 2926, 1710, and 1462 cm^{-1}. Tween®80 exhibited peaks at 2908, 2954, and 1736 cm^{-1}, whereas Eudragit S100 exhibited characteristic peaks at 2954, 1730,

Table II. Composition of Check Point Batch and Its Recorded Responses

Batch no.	X_1 (mg)	X_2 (%)	Parameters	Particle size (nm)	EE (%)
P10	73.925	1.498	Observed value	101.7 ± 1.32	83.50 ± 2.4%
			Predicted value	100.234	84.82
			% Error	1.46	1.55

and 1452 cm^{-1}. In the EU-5-FU-NLCs spectrum, peaks at similar band groups can be observed, which suggests that there was no chemical interaction between the active and NLC excipients. The variation in the peak intensities could be attributed to the overlapping of certain functional groups for the specific bandwidth (44).

Differential Scanning Calorimetry. DSC provides information about the amorphous or crystalline nature of a given sample. DSC analysis was performed for 5-FU and EU-5-FU-NLCs. Thermograms of 5-FU (Fig. 5a) exhibited a sharp melting endotherm at 289.89°C, coinciding with its melting point and indicating its crystalline nature. In the thermogram of EU-5-FU-NLCs (Fig. 5b), the peak of 5-FU was not present indicating molecular dispersion of 5-FU into the lipid and conversion from crystalline to amorphous nature (17).

X-ray Diffraction. The X-ray diffractograms of 5-FU (Fig. 5c) displayed a sharp peak at 2θ equals 20.87° qualifying its crystalline nature. The characteristic peaks corresponding to 5-FU were absent in the diffractograms of EU-5-FU-NLCs (Fig. 5d). This could be due to the conversion of the crystalline 5-FU into its amorphous counterpart during the formulation of EU-5-FU-NLCs (17).

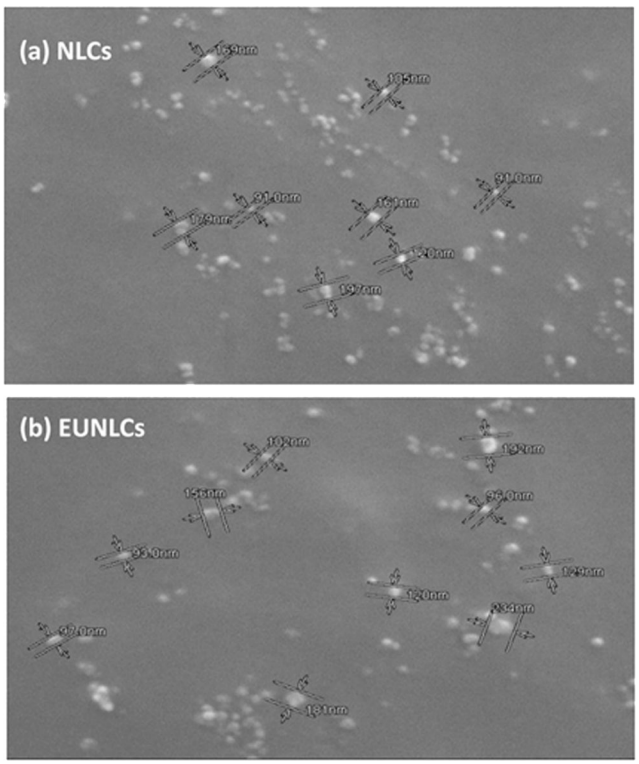

Figure 3. SEM image. **a** 5-FU-NLC and **b** EU-5-FU-NLCs

In Vitro Drug Release Study. In vitro release of 5-FU from 5-FU-DS, 5-FU-NLCs, and EU-5-FU-NLCs was carried out using change over media to evaluate the pH sensitivity of the formulation. The *in vitro* drug release profiles of all three formulations are depicted in Fig. 6. The drug release from 5-FU-DS, 5-FU-NLCs, and EU-5-FU-NLCs at the end of 2 h was found to be 100%, 35.33%, and 2.36%, respectively. The values suggested complete release from the5-FU-DS, whereas the nanoformulations exhibited a slower rate of release, which is due to the presence of 5-FU in the lipidic matrix. Initial burst release (35.33%) of drug from 5-FU-NLCs might be due to some non-entrapped drug on the surface of nanoparticles. It was clear from the 2-h release data from EU-5-FU-NLCs that the surface modification of 5-FU-NLCs with pH-sensitive polymer-Eudragit S100 was able to protect the drug from the harsh environment of gastric fluid and retard its release into the acidic milieu (15).

At the end of 4 h of release in acetate buffer media (pH 4.5), the release from 5-FU-NLCs, and EU-5-FU-NLCs was 69.04% and 9.95%, respectively. In the case of 5-FU-NLCs, the values are suggestive of major amount of active being released in the proximal part of the small intestine, whereas no significant drug release occurred from EU-5-FU-NLCs in pH 4.5 as well.

After acetate buffer (pH 4.5), the release was carried out in phosphate buffer media (pH 7.4). Only 30% of 5-FU was remaining to be released from 5-FU-NLCs, whereas 90% of 5-FU was remaining to be released from EU-5-FU-NLCs. The major amount of drug release from EU-5-FU-NLCs began only after exposure to pH 7.4. This could be attributed to the presence of carboxyl groups in Eudragit S100 polymer that ionize when there is a pH shift from acidic to alkaline. At alkaline pH, ionization takes place that disturbs the integrity of the coat, and 5-FU starts leaching from the nanoparticles (45). Furthermore, the release of the active from EU-5-FU-NLCs occurred in a controlled fashion requiring 24 h for the complete release. The controlled release of 5-FU could be attributed due to the presence of the active inside the core of the lipid matrix of NLC which undergoes slow erosion. The controlled release profile of 5-FU from EU-5-FU-NLCs observed in our study corroborated well with those reported previously in addition to the negligible release of 5-FU at lower pH (1–2) as compared to previously reported studies (3,15,17).

This kind of spatial and temporal release pattern of 5-FU is of great clinical interest for the management of colon cancer in the view that steady release is provided over a prolonged period at the site of action.

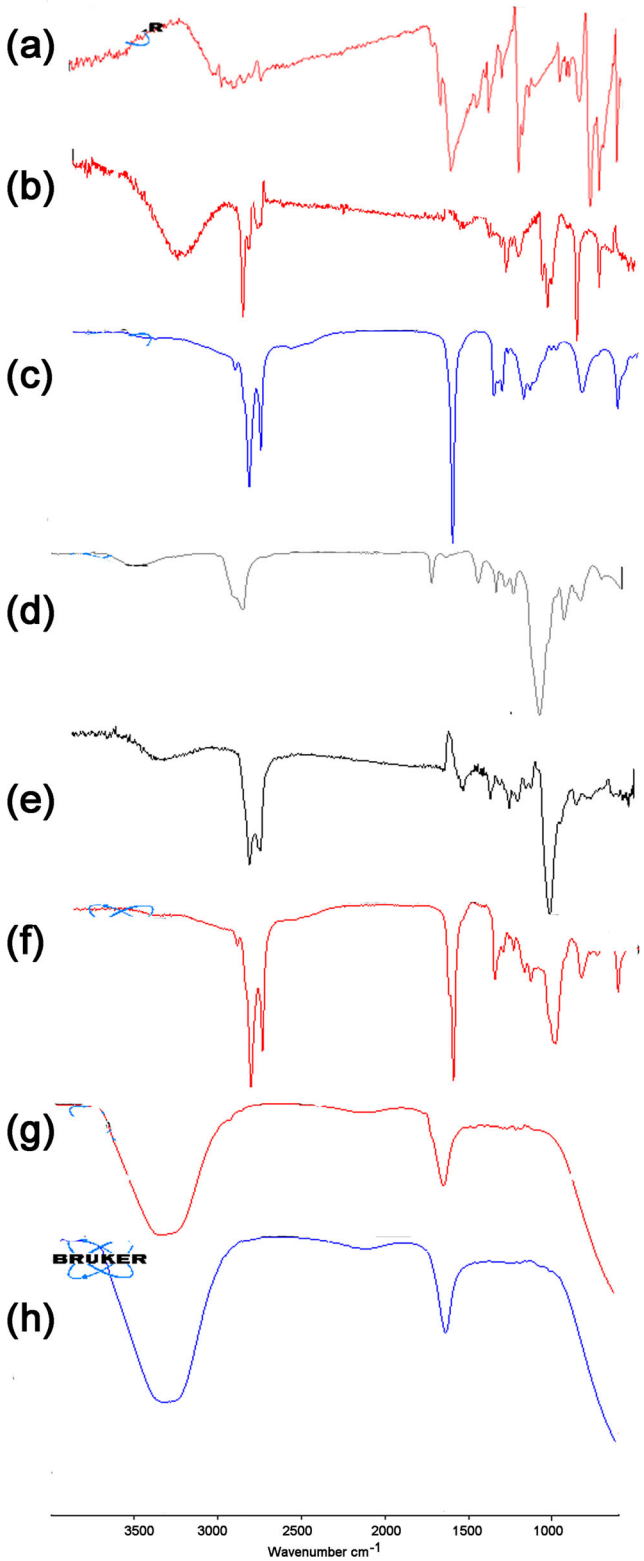

Figure 4. FTIR spectra of **a** 5-FU, **b** Compritol®ATO 888, **c** oleic acid, **d** Tween 80, **e** Eudragit S100, **f** physical mixtures, **g** 5-FU-NLCs, and **h** EU-5-FU-NLCs

Ex Vivo Release Study. In this study, we measured the amount of 5-FU transported from 5-FU-DS and EU-5-FU-NLCs across the colonic barrier using the non-everted gut-sac method. The amount of 5-FU transported from the formulations at pH 7.4 has been shown in Fig. 7. At the end of 24 h, release from 5-FU-DS was only 50%, whereas EU-5-FU-NLCs could release 100% of 5-FU. Thus, a significant amount of 5-FU was transported across the colonic barrier from EU-5-FU-NLCs as compared to 5-FU-DS. In the case of *in vitro* study, rapid and complete release of 5-FU occurred from 5-FU-DS, whereas only partial and slow release occurred in case of *ex vivo* study. This might be attributed to apically directed efflux transporter, P-gp, which attenuates the absorptive and enhances the secretory transport of 5-FU across the intestinal epithelium. In the case of EU-5-FU-NLCs, the augmentation of absorptive transport might be attributed to the inhibitory activities of Tween®80 and Eudragit S100 on the P-gp efflux pump.

The release pattern of EU-5-FU-NLCs was as follows: 7.40 ± 2.19% (after 2 h), 26.5 ± 4.45% (after 6 h), and 100.90 ± 3.96% (after 24 h). The release of 5-FU occurred in a controlled fashion, which is due to the lipidic matrix formed by the presence of solid and liquid lipids.

Ex vivo release data from EU-5-FU-NLCs was subjected to goodness-of-fit test by linear regression analysis according to zero order, first order, Higuchi, Hixon-Crowell, and Korsmeyer-Peppas models to ascertain the kinetics and mechanism of drug release. The R^2 values for zero order, first order, Higuchi, Hixon-Crowell, and Korsmeyer-Peppas models were found to be 0.9978, 0.9304, 0.8359, 0.9976, and 0.9600, respectively. Based on the R^2 value, EU-5-FU-NLCs were found to exhibit zero-order release kinetics, indicating the controlled release nature of the developed nanomatrix formulation. The value of n characterizes the release mechanism of the drug. For the present case, n was 0.996, indicative of non Fickian diffusion, as a combination of both diffusion and erosion controlled rate release (46).

In Vitro Cytotoxicity assay. The cytotoxicity of blank EU-NLCs, 5-FU-DS, 5-FU-NLCs, and EU-5-FU-NLCs was carried out by MTT assay in Caco-2 cells. The cell viability of blank EU-NLCs was found to be 99% indicating the safety of the excipients employed in the NLC formulation. 5-FU-DS, 5-FU-NLCs, and EU-5-FU-NLCs exhibited dose-dependent cytotoxicity. The cell viabilities at 1, 10, and 100 μM concentrations were estimated, and the results are represented in Fig. 8. The results revealed that the viability of cells was inversely proportional to the concentration of 5-FU in each of the formulations. Among the three formulations, the viability of cells exposed to 5-FU-DS was significantly ($P < 0.05$) higher than those exposed to 5-FU-NLCs and EU-5-FU-NLCs. This could be attributed to the inability of 5-FU from 5-FU-DS to internalize the cells due to the P-gp efflux. The higher cytotoxicity activity associated with 5-FU-NLCs and EU-5-FU-NLCs could be explained by the enhanced permeation and retention effect due to the inhibition of P-gp efflux by efflux inhibitors such as Tween®80 and Eudragit S100 (4,47,48). Thus, P-gp substrates like 5-FU can be delivered efficiently inside the cancerous cell through the use of nanoformulations (15).

In Vivo Study. Plasma concentration-time profiles of the 5-FU solution, (group I), 5-FU-NLCs (group II), and EU-5-

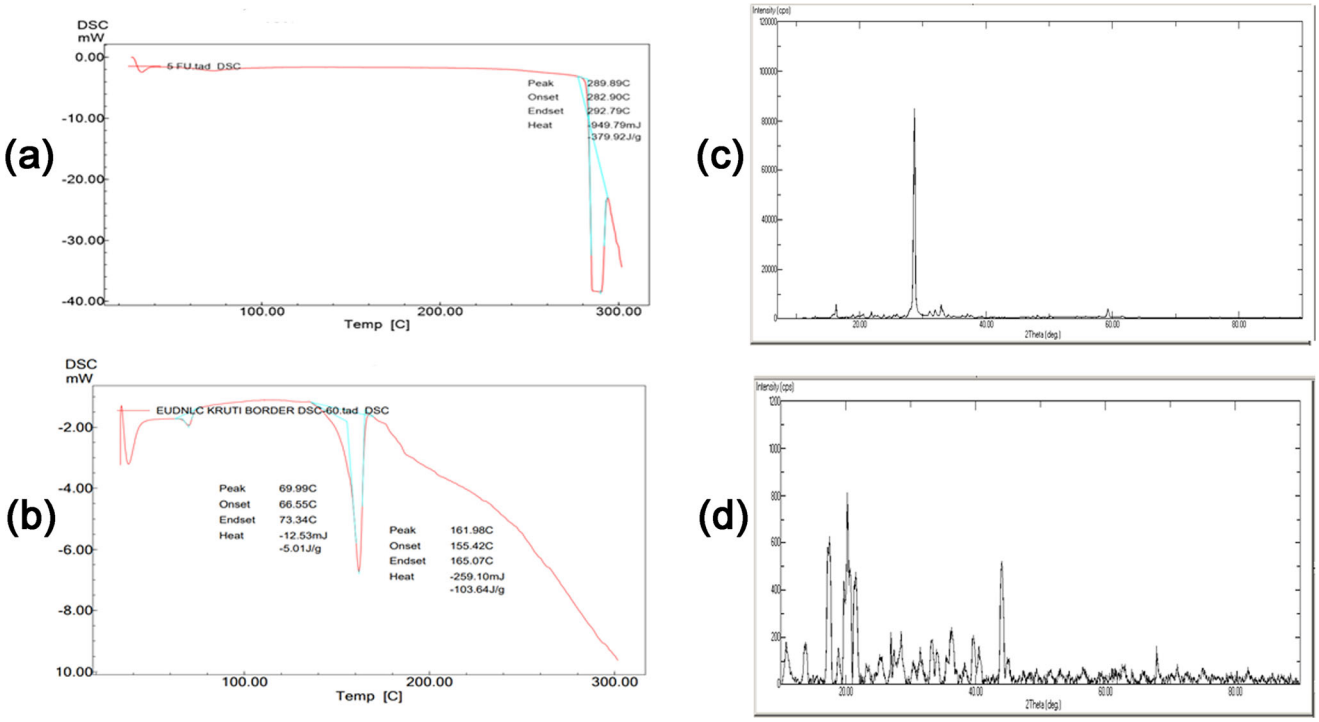

Figure 5. **a** DSC thermogram of 5-FU. **b** DSC thermogram of EU-5-FU-NLCs. **c** XRD spectrum of 5-FU. **d** XRD spectrum of EU-5-FU-NLCs

FU-NLCs (group III) were obtained and shown in Fig. 9. The calculated pharmacokinetic parameters are tabulated in Table III. The drug appeared immediately in plasma upon administration of 5-FU-DS (T_{max} = 0.5 hours) and was detected only up to 6 h, indicating a quick decrease in the plasma levels. Our findings are in accordance with the results of Li et al. (11) and Subudhi et al. (15). On the other hand, the T_{max} values for 5-FU-NLCs and EU-5-FU-NLCs were found to be 4 h and 8 h, respectively. Both uncoated and coated nanoformulations indicated a significant (p<0.05) prolongation in T_{max} owing to the slow release of the drug from the formulation. The coated NLCs indicated a further delay in T_{max} which could be attributed to the efficient coating with Eudragit S100 that hinders the release of 5-FU in the upper part of the GI tract and releases it in the colon. The plasma concentration of EU-5-FU-NLCs decreased gradually over the next 16 h indicating a prolonged residence time of 5-FU in the colon. This could be because degradation of pH-sensitive polymer (Eudragit S100) by colonic microflora is a slow process that requires several hours for completion (49). Such a slow and constant drug input is beneficial to cancer therapy in the case of drugs with short plasma half-lives. The MRT of 5-FU from 5-FU-DS, 5-FU-NLCs, and EU-5-FU-NLCs were found to be 3.04± 0.72 h, 8.27 ± 0.99 h, and 13.13± 1.04, respectively. A 4.32 fold relative increase in MRT of 5-FU from EU-5-FU-NLCs in comparison to 5-FU-DS further confirmed the sustained release characteristics of the surface modified nanoformulation (43). The results of T_{max} and MRT are consistent with the *in vitro* release of 5-FU from the formulations.

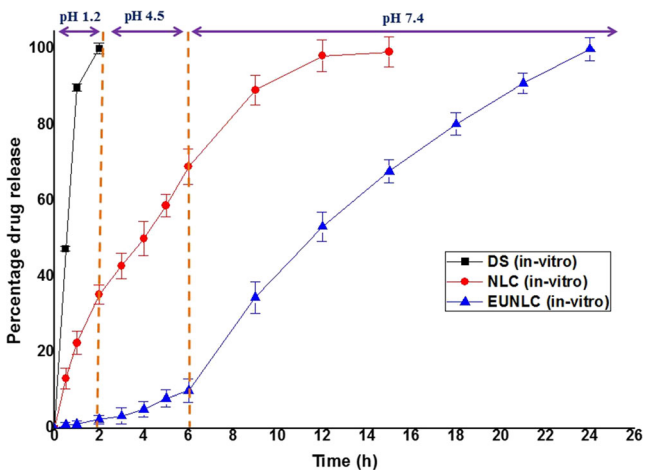

Figure 6. *In vitro* release profile of 5-FU-DS, 5-FU-NLCs, and EU-5-FU-NLCs

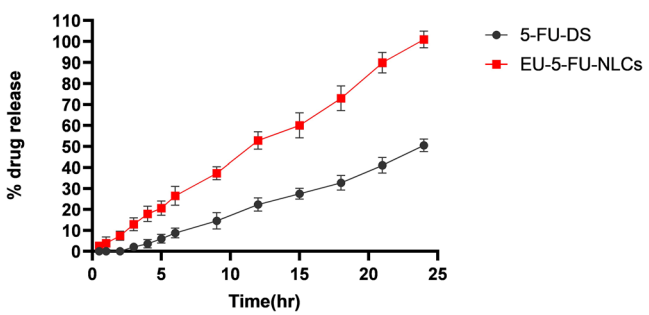

Figure 7. *Ex vivo* release profile of 5-FU-DS, 5-FU-NLCs, and EU-5-FU-NLCs

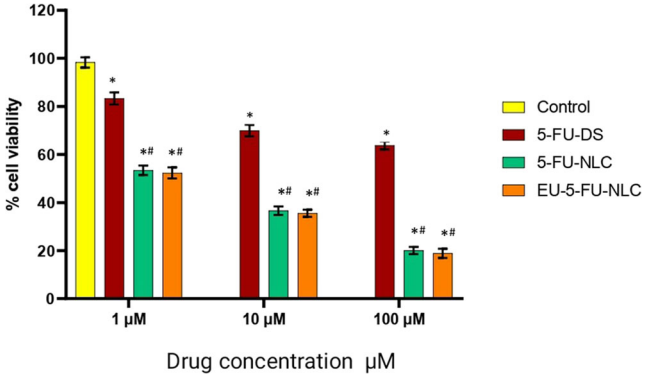

Figure 8. MTT assay of 5-FU-DS, 5-FU-NLCs, EU-blank NLCs, and EU-5-FU-NLCs

5-FU-DS, 5-FU-NLCs, and EU-5-FU-NLCs exhibited C_{max} values of 6.76± 1.98 µg/mL, 14.39± 2.33µg/mL, and 17.27± 2.04µg/mL, respectively. AUC_{0-t} of 5-FU DS, 5-FU-NLCs, and EU-5-FU-NLCs were recorded as 16.81 ± 4.66 µg·h/mL, 84.30 ± 5.16 µg.h/mL, and 185.26 ± 13.13 µ·h/mL, respectively, and both were extremely significant ($P < 0.001$) as compared to 5-FU DS. The size of the AUC value can reflect the size of the bioavailability. Based on the AUC values, the relative bioavailability of 5-FU-NLCs and EU-5-FU-NLCs were found to increase by 5 and 11 folds, respectively, compared to plain drug solution. The low bioavailability of 5-FU is due to its low GI permeability, P-gp efflux, inconsistent absorption in the gastrointestinal tract, and hepatic first-pass metabolism (50). Higher bioavailability (C_{max}, AUC) of 5-FU-NLCs may be due to maximum delayed release of drug bypassing the gastric fluids and due to the clathrin-mediated endocytosis (particle size < 200 nm) (51). However, the uncoated nanoparticles release majority of 5-FU in the intestine, where it shows slow absorption due to low permeability (49) and undergoes intestinal first-pass metabolism (52), resulting in bioavailability significantly lower than the EU-5-FU-NLCs. The highest bioavailability achieved with EU-5-FU-NLCs was attributed to the pH-sensitive character of Eudragit S100, which decreased the absorption in the intestinal tract and reduced the first-pass metabolism of 5-FU in the liver and intestine. Additionally, Tween®80 and Eudragit S100 are known P-gp inhibitors reducing the efflux of P-gp substrate-5-FU (47,48).

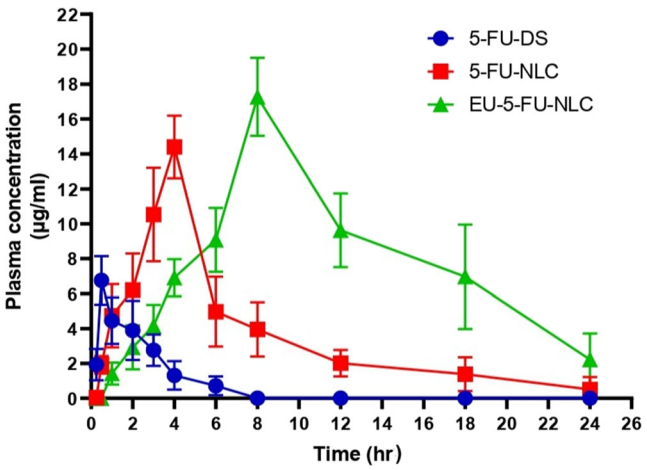

Figure 9. Pharmacokinetic parameters of 5-FU-DS, 5-FU-NLCs, and EU-5-FU-NLC after oral administration in Albino Wistar rats

The higher bioavailability along with significantly prolonged retention of EU-5-FU-NLCs *in vivo* accounts for a higher amount of 5-FU being available for interaction at the target site in the colonic tissue for a longer duration. The pharmacokinetic parameters prove the ability of developed EU-5-FU-NLCs as a novel site-specific carrier for 5-FU with the ability to deliver the maximum amount of drug to the colon while minimizing drug absorption in the early parts of the GI tract. A significant improvement in oral bioavailability of 5-FU via surfaced modified NLC by use of pH-sensitive polymer (Eudragit S100) compared to free drug solution and plain nanoparticles could lead to reduction in the dose, dose-related side effects, and cost of the therapy providing increased patient compliance.

Stability Study. Stability is a very crucial aspect of any formulation influencing its safety and efficacy across the shelf life. Nanoformulations are reported to possess a shorter shelf life in comparison to their conventional counterparts; however, their proven efficacy had led them to gain importance. Stability study of EU-5-FU-NLCs was carried out at 4°C and 25°C. The results are depicted in Table IV. EU-5-FU-NLCs were evaluated at the 10th, 20th, and 30th day for any changes in particle size and entrapment efficiency. At refrigerated conditions, an increase in particle size occurred from 154.0 ± 3.17 to 157.1 ± 3.61 nm, whereas % EE changed from 89.81 ± 2.60% to 87.23 ± 1.85%. On the other hand, at room temperature, an increase in particle size occurred from 154.0 ± 3.17 to 166.2 ± 2.99 nm, whereas % EE decreased from 89.81 ± 2.60% to 83.30± 2.09%. The results indicated a non-significant (P>0.05) change in particle size and entrapment efficiency of EU-5-FU-NLCs when stored at 4°C; whereas both the parameters changed significantly (P<0.05) upon its storage at 25°C, a statistically significant difference in % EE. was noticed. Thus, due to the higher stability, the suggested storage for EU-5-FU-NLC is 2–8°C. These results are in agreement with Elmowafy et al. (53) who studied the effect of temperature on the stability of Atorvastatin-loaded NLCs.

CONCLUSION

5-FU-loaded nanostructured lipid carriers were formulated by the HPH technique. Higher entrapment efficiency (>80%) and lower particle size (<200 nm) were achieved by optimization of the critical material attributes through a 3^2 factorial design. pH-sensitive NLCs were successfully fabricated by the surface modification of optimized 5-FU-NLCs with Eudragit S100. *In vitro* and *in vivo* studies confirmed the ability of EU-5-FU-NLCs to retain the integrity of the nanometric formulation and protect the 5-FU-embedded NLCs to pass through the stomach and intestine without releasing the drug. 5-FU from EU-5-FU-NLCs was exposed to the colon once the Eudragit S100 coating was dissolved. Further, the release

Table III. Pharmacokinetic Parameters of 5-FU, 5-FU-NLC, and EU-5-FU-NLC After Oral Administration in Albino Wistar Rats

Parameter	5-FU-DS	5-FU-NLC	EU-5-FU-NLC
Time to achieve maximum concentration (T_{max}) (h)	0.5	4	8
Mean residence time (MRT) (h)	3.04	8.26	13.13
Maximum concentration achieved (C_{max}) (μg/ml)	6.76 ± 1.98	14.39 ± 2.33	17.27 ± 2.04
Area under curve (AUC_{0-t}) (μg·h/ml)	16.81 ± 4.66	84.30 ± 5.16	185.26 ± 13.13
Area under curve ($AUC_{0-\infty}$) (μg·h/ml)	18.10 ± 5.07	88.51 ± 6.03	203.85 ± 15.18
Relative bioavailability (Fr) (folds)		5.01	11.02

Table IV. Stability Studies of EU-5-FU-NLCs at 4 ± 1°C and 25 ± 1°C After 1-Month Storage

Particle size (nm)							% EE						
0 day	10 days		20 days		30 days		0 day	10 days		20 days		30 days	
	4 ± 1°C	25 ± 1°C	4 ± 1°C	25 ± 1°C	4 ± 1°C	25 ± 1°C		4 ± 1°C	25 ± 1°C	4 ± 1°C	25 ± 1°C	4 ± 1°C	25 ± 1°C
154.0 ± 3.17	154.9 ± 2.20	156.1 ±4.11	156.3 ± 4.07	160.5 ± 3.54	157.1 ± 3.61	166.2 ± 2.99	89.81 ± 2.60	89.11 ± 2.44	87.09 ± 2.18	88.47 ± 1.97	85.66 ± 2.13	87.23 ± 1.85	83.30 ± 2.09

of the drug occurred in a sustained fashion due to the lipid matrix. Therefore, this kind of drug delivery system has the potential of providing spatial and temporal release of 5-FU in the chemotherapy of colon cancer. However, extensive pharmacokinetic, pharmacodynamic, and chronic toxicity studies are needed before establishing this novel drug delivery system from the bench to the bedside.

SUPPLEMENTARY INFORMATION

The online version contains supplementary material available at https://doi.org/10.1208/s12249-021-02099-3.

ACKNOWLEDGEMENTS

The authors would like to acknowledge the Maliba Pharmacy College for providing facilities to perform the experimental work and financial assistance for this study.

AUTHOR CONTRIBUTION

Kruti Borderwala: data collection. Sachin Rathod: data collection. Sarita Yadav: draft manuscript preparation. Bhavin Vyas: analysis and interpretation of results. Pranav Shah: study conception and design. All the authors reviewed the results and approved the final version of the manuscript.

DECLARATIONS

Conflict of Interest The authors declare no competing interests.

REFERENCES

1. Ramanathan RK, Clark JW, Kemeny NE, Lenz H-J, Gococo KO, Haller DG, et al. Safety and toxicity analysis of oxaliplatin combined with fluorouracil or as a single agent in patients with previously treated advanced colorectal cancer. J Clin Oncol. 2003;21:2904–11.
2. Dhawale SC, Bankar AS, Patro MN. Formulation and evaluation porous microspheres of 5-fluorouracil for colon targeting. Int J Pharm Tech Res. 2010;2:1112–8.
3. Khatik R, Mishra R, Verma A, Dwivedi P, Kumar V, Gupta V, et al. Colon-specific delivery of curcumin by exploiting Eudragit-decorated chitosan nanoparticles in vitro and in vivo. J Nanopart Res. 2013;15:1–15.
4. Tummala S, Gowthamarajan K, Satish Kumar MN, Wadhwani A. Oxaliplatin immuno hybrid nanoparticles for active targeting: an approach for enhanced apoptotic activity and drug delivery to colorectal tumors. Drug Deliv. 2016;23:1773–87.
5. Lamprecht A, Yamamoto H, Takeuchi H, Kawashima Y. Observations in simultaneous microencapsulation of 5-fluorouracil and leucovorin for combined pH-dependent release. Eur J Pharm Biopharm. 2005;59:367–71.
6. Arias JL. Novel strategies to improve the anticancer action of 5-fluorouracil by using drug delivery systems. Molecules. 2008;13:2340–69.
7. Dong Y, Feng S-S. In vitro and in vivo evaluation of methoxy polyethylene glycol–polylactide (MPEG–PLA) nanoparticles for small-molecule drug chemotherapy. Biomaterials. 2007;28:4154–60.
8. Zhang N, Yin Y, Xu S-J, Chen W-S. 5-Fluorouracil: mechanisms of resistance and reversal strategies. Molecules. 2008;13:1551–69.
9. Shimono N, Takatori T, Ueda M, Mori M, Higashi Y, Nakamura Y. Chitosan dispersed system for colon-specific drug delivery. Int J Pharm. 2002;245:45–54.

10. Zhang J, Wang X, Liu T, Liu S, Jing X. Antitumor activity of electrospun polylactide nanofibers loaded with 5-fluorouracil and oxaliplatin against colorectal cancer. Drug Deliv. 2016;23:784–90.
11. Li P, Yang Z, Wang Y, Peng Z, Li S, Kong L, et al. Microencapsulation of coupled folate and chitosan nanoparticles for targeted delivery of combination drugs to colon. J Microencapsul. 2015;32:40–5.
12. van Kuilenburg AB, Maring JG. Evaluation of 5-fluorouracil pharmacokinetic models and therapeutic drug monitoring in cancer patients. Pharmacogenomics. 2013;14:799–811.
13. Nakayama Y, Matsumoto K, Inoue Y, Katsuki T, Kadowaki K, Shibao K, et al. Correlation between the urinary dihydrouracil-uracil ratio and the 5-FU plasma concentration in patients treated with oral 5-FU analogs. Anticancer Res. 2006;26:3983–8.
14. Rai G, Yadav AK, Jain NK, Agrawal GP. Eudragit-coated dextran microspheres of 5-fluorouracil for site-specific delivery to colon. Drug Deliv. 2016;23:328–37.
15. Subudhi MB, Jain A, Jain A, Hurkat P, Shilpi S, Gulbake A, et al. Eudragit S100 coated citrus pectin nanoparticles for colon targeting of 5-fluorouracil. Materials (Basel). 2015;8:832–49.
16. Patil-Gadhe A, Pokharkar V. Montelukast-loaded nanostructured lipid carriers: part I oral bioavailability improvement. Eur J Pharm Biopharm. 2014;88:160–8.
17. Tummala S, Kumar MNS, Prakash A. Formulation and characterization of 5-Fluorouracil enteric coated nanoparticles for sustained and localized release in treating colorectal cancer. Saudi Pharm J. 2015;23:308–14.
18. Sutar PS, Joshi VJ. Preparation and characterisation of 5-fluorouracil loaded PLGA nanoparticles for colorectal cancer therapy. Unique J Pharm Biol Sci. 2013;1(2):52–8.
19. Varshosaz J, Hassanzadeh F, Sadeghi H, Khadem M. Galactosylated nanostructured lipid carriers for delivery of 5-FU to hepatocellular carcinoma. J Liposome Res. 2012;22:224–36.
20. Qu C-Y, Zhou M, Chen Y, Chen M, Shen F, Xu L-M. Engineering of lipid prodrug-based, hyaluronic acid-decorated nanostructured lipid carriers platform for 5-fluorouracil and cisplatin combination gastric cancer therapy. Int J Nanomedicine. 2015;10:3911–20.
21. Rajinikanth PS, Chellian J. Development and evaluation of nanostructured lipid carrier-based hydrogel for topical delivery of 5-fluorouracil. Int J Nanomedicine. 2016;11:5067–77.
22. Luan J, Zhang D, Hao L, Qi L, Liu X, Guo H, et al. Preparation, characterization and pharmacokinetics of Amoitone B-loaded long circulating nanostructured lipid carriers. Colloids Surf B: Biointerfaces. 2014;114:255–60.
23. Andalib S, Varshosaz J, Hassanzadeh F, Sadeghi H. Optimization of LDL targeted nanostructured lipid carriers of 5-FU by a full factorial design. Adv Biomed Res. 2012;1:45.
24. Kim MH, Kim KT, Sohn SY, Lee JY, Lee CH, Yang H, et al. Formulation and evaluation of nanostructured lipid carriers (NLCs) of 20(S)-protopanaxadiol (PPD) by Box-Behnken design. Int J Nanomedicine. 2019;14:8509–20.
25. Shah P, Chavda K, Vyas B, Patel S. Formulation development of linagliptin solid lipid nanoparticles for oral bioavailability enhancement: role of P-gp inhibition. Drug Deliv and Transl Res. 2021;11:1166–85.
26. Kasongo KW, Müller RH, Walker RB. The use of hot and cold high pressure homogenization to enhance the loading capacity and encapsulation efficiency of nanostructured lipid carriers for the hydrophilic antiretroviral drug, didanosine for potential administration to paediatric patients. Pharm Dev Technol. 2012;17(3):353–62.
27. Mahdi WA, Hussain A, Ramzan M. 5-Fluorouracil loaded biogenic and albumin capped gold nanoparticles using bacterial enzyme—in vitro-in silico Gastroplus® simulation and prediction. Processes. 2020;8:1579.
28. Lalan M, Shah P, Shah K, Prasad A. Developmental studies of curcumin NLCs as safe alternative in management of infectious childhood dermatitis. Nanoscience & Nanotechnology-Asia. 2020;10(4):390–403.
29. Shah P, Dubey P, Vyas B, Kaul A, Mishra AK, Chopra D, et al. Lamotrigine loaded PLGA nanoparticles intended for direct nose to brain delivery in epilepsy: pharmacokinetic, pharmacodynamic and scintigraphy study. Artificial Cells, Nanomedicine, and Biotechnology. 2021;49(1):511–22.
30. Naik B, Gandhi J, Shah P, Naik H, Sarolia J. Asenapine maleate loaded solid lipid nanoparticles for oral delivery. International Research Journal of Pharmacy. 2017;8:45–53.
31. Shah P, Sarolia J, Vyas B, Wagh P, Kaul A, Mishra AK. PLGA Nanoparticles for nose to brain delivery of clonazepam: formulation, optimization by 3^2 factorial design, In vitro and In vivo Evaluation. Curr Drug Deliv. 2021;17. https://doi.org/10.2174/1567201817666200708115627.
32. Borderwala K, Swain G, Mange N, Gandhi J, Lalan M, Singhvi G, et al. Optimization of solid lipid nanoparticles of ezetimibe in combination with simvastatin using quality by design (QbD). Nanoscience & Nanotechnology-Asia. 2020;10(4):404–18.
33. Mahdi ZS, Roshan FT, Nikzad M, Ezoji H. Biosynthesis of zinc oxide nanoparticles using bacteria: a study on the characterization and application for electrochemical determination of bisphenol A. Inorg Nano-Met Chem. 2020:1–9. https://doi.org/10.1080/24701556.2020.1835962.
34. El-Badry M, Fetih G, Fathy M. Improvement of solubility and dissolution rate of indomethacin by solid dispersions in Gelucire 50/13 and PEG4000. Saudi Pharmaceutical Journal. 2009;17(3):217–25.
35. Bayat A, Dorkoosh FA, Dehpour AR, Moezi L, Larijani B, Junginger HE, et al. Nanoparticles of quaternized chitosan derivatives as a carrier for colon delivery of insulin: ex vivo and in vivo studies. Int J Pharm. 2008;356(1-2):259–66.
36. Dash V, Mishra SK, Singh M, Goyal AK, Rath G. Release kinetic studies of aspirin microcapsules from ethyl cellulose, cellulose acetate phthalate and their mixtures by emulsion solvent evaporation method. Sci Pharm. 2010;78:93–102.
37. Sinha VR, Kumar RV, Bhinge JR. A stability-indicating RP-HPLC assay method for 5-fluorouracil. Indian J Pharm Sci. 2009;71(6):630–7.
38. Alam T, Khan S, Gaba B, Haider MF, Baboota S, Ali J. Adaptation of quality by design based development of isradipine nanostructured–lipid carrier and its evaluation for in vitro gut permeation and in vivo solubilization fate. J Pharm Sci. 2018;107(11):2914–26.
39. Pathak BK, Raghav M, Thakkar AR, Vyas BA, Shah PJ. Enhanced oral bioavailability of etodolac by the liquisolid compact technique: optimisation, in-vitro and in-vivo evaluation. Current Drug Delivery. 2021;18(4):471–86.
40. Agrawal Y, Petkar KC, Sawant KK. Development, evaluation and clinical studies of Acitretin loaded nanostructured lipid carriers for topical treatment of psoriasis. Int J Pharm. 2010;401(1-2):93–102.
41. Shah NV, Seth AK, Balaraman R, Aundhia CJ, Maheshwari RA, Parmar GR. Nanostructured lipid carriers for oral bioavailability enhancement of raloxifene: design and in vivo study. J Adv Res. 2016;7(3):423–34.
42. Ahad A, Aqil A, Kohli K, Sultana Y, Mujeeb M, Ali A. Formulation and optimization of nanotransfersomes using experimental design technique for accentuated transdermal delivery of valsartan. Nanomedicine. 2012;8(2):237–49.
43. Anwer MK, Mohammad M, Ezzeldin E, Fatima F, Alalaiwe A, Iqbal M. Preparation of sustained release apremilast-loaded PLGA nanoparticles: in vitro characterization and in vivo pharmacokinetic study in rats. Int J Nanomedicine. 2019;14:1587–95.
44. Nagarwal RC, Singh PN, Kant S, Maiti P, Pandit JK. Chitosan nanoparticles of 5-fluorouracil for ophthalmic delivery: characterization, in-vitro and in-vivo study. Chem Pharm Bull (Tokyo). 2011;59(2):272–8.
45. Sharma VK, Jain A, Soni V. Nano-aggregates: emerging delivery tools for tumor therapy. Crit Rev Ther Drug Carrier Syst. 2013;30:535–63.
46. Nagaich U, Gulati N. Nanostructured lipid carriers (NLC) based controlled release topical gel of clobetasol propionate: design and in vivo characterization. Drug Deliv Transl Res. 2016;6(3):289–98.
47. Zhang H, Yao M, Morrison RA, Chong S. Commonly used surfactant, Tween 80, improves absorption of P-glycoprotein substrate, digoxin, in rats. Arch Pharm Res. 2003;26:768–72.

48. Mohammadzadeh R, Baradaran B, Valizadeh H, Yousefi B, Zakeri-Milani P. Reduced ABCB1 expression and activity in the presence of acrylic copolymers. Adv Pharm Bull. 2014;4(3):219–24.
49. Wei H, Qing D, De-Ying C, Bai X. Fanli-Fang. Pectin/ethylcellulose as film coatings for colon-specific drug delivery: preparation and in vitro evaluation using 5-fluorouracil pellets. PDA J Pharm Sci Technol. 2007;61(2):121–30.
50. El-Hammadi MM, Delgado ÁV, Melguizo C, Prados JC, Arias JL. Folic acid-decorated and PEGylated PLGA nanoparticles for improving the antitumour activity of 5-fluorouracil. Int J Pharm. 2017;516(1-2):61–70.
51. Beloqui A, Solinís MA, Gascón AR, del Pozo-Rodríguez A, des Rieux A, Préat V. Mechanism of transport of saquinavir-loaded nanostructured lipid carriers across the intestinal barrier. J Control Release. 2013;166(2):115–23.
52. Gu J, Yuasa H, Hayashi Y, Watanabe J. First-pass metabolism of 5-fluorouracil in the perfused rat small intestine. Biol Pharm Bull. 1998;21(8):871–3.
53. Elmowafy M, Ibrahim HM, Ahmed MA, Shalaby K, Salama A, Hefesha H. Atorvastatin-loaded nanostructured lipid carriers (NLCs): strategy to overcome oral delivery drawbacks. Drug Deliv. 2017;24(1):932–41.